

On Baryogenesis and $n\bar{n}$ -Oscillations

Enrico Herrmann*

*Walter Burke Institute for Theoretical Physics,
California Institute of Technology, Pasadena, CA 91125*

(Dated: August 21, 2014)

We study a simple model where color sextet scalars violate baryon number at tree level but do not give rise to proton decay. In particular, we include one light and two heavy sextets with $\Delta B = 2$ baryon number violating interactions that induce neutron anti-neutron oscillations. This setup also suggests an intimate connection to the generation of the observed baryon asymmetry in the Universe via the out of equilibrium decay of the heavy sextet scalars at around 10^{14} GeV. The large $SU(3)$ -color charges of the scalar fields involved in generating the baryon asymmetry motivate us to study potentially significant washout effects. We numerically solve a set of Boltzmann evolution equations and find restrictions on the available model parameters imposed by successful high scale baryogenesis. Combining our new numerical results for baryogenesis with $n\bar{n}$ -oscillation predictions and collider limits on the light sextet, we identify parameter regions where this model can be probed by current and future experiments.

I. INTRODUCTION

The origin of the baryon asymmetry in the Universe (BAU) is one of the major open puzzles not solved within the Standard Model of particle physics. Over the years, a wide range of models and mechanisms to generate the observed baryon asymmetry have been suggested. Electroweak baryogenesis [1], baryogenesis via leptogenesis [2], the Affleck-Dine mechanism [3] and GUT-baryogenesis [4] are some of the most common representatives. For a comprehensive review, we encourage the reader to consult e.g. [5] and references therein.

In 1967, Sakharov [6] formulated three necessary ingredients for successful baryogenesis: 1) CP -violation, 2) baryon number violation and 3) the deviation from thermal equilibrium. Perturbatively, the Standard Model preserves baryon-number, but this accidental global symmetry is anomalous at the quantum level. In principle, the Standard Model contains all required ingredients to generate a baryon asymmetry. However it was shown that the attainable asymmetry is inconsistent with observation [7]. Beyond the Standard Model there are a variety of well motivated extensions (e.g. [8–10]) that introduce new interactions which violate baryon number classically. Generically, this leads to proton decay which is tightly constrained by experiment [11]. In this article, we discuss a minimal model, suggested in [12], that violates baryon number in such a way that the proton decay channel is absent and $n\bar{n}$ -oscillations become the primary signal of baryon number violating physics. In particular, we consider the situation where one light (X_1) and one heavy (X_2) color sextet scalar field mediate these interactions.

One attractive feature of this scenario is the possibility to integrate our simplified model into a complete non-supersymmetric grand unified theory in the spirit of Ref. [13].

There, one of the color sextets is kept at the TeV-scale to ensure gauge coupling unification.

Building on the discussions in Refs. [12, 13] we show that the model is able to accommodate successful high-scale baryogenesis as well as $n\bar{n}$ -oscillations with discovery potential at the European Spallation Source (ESS)¹ [14]. However the preferred parameter regions for the two effects are in some tension (c.f. results in Sec. III C and Sec. IV). We perform a detailed analysis of the baryogenesis setup beyond the approximate decay scenarios assumed in the literature [12, 13] by numerically solving the Boltzmann equations to track the relevant particle densities in the early Universe. This way, we correctly take into account potentially large washout contributions due to the sizable color charge of the new scalars. We also consider collider limits on new colored particles from LHC-searches that have been analyzed for color sextets in Ref. [15].

The remainder of this note is structured as follows: In section II we introduce the field content and the parameters of our model which are relevant for the discussion of baryogenesis and $n\bar{n}$ -oscillations. In section III we rehash some facts about baryogenesis before writing down the Boltzmann equations in subsection III A. We also compute the relevant scattering- and decay-rates that feed into these equations. Subsequently, we discuss $n\bar{n}$ -oscillations in section IV and show how to combine this with successful baryogenesis. This allows us to analyze the two phenomena in terms of physically motivated quantities and measurable parameters only. Additional signals and constraints of our model, such as collider signatures, contributions to the neutron electric dipole moment (Sec. V) as well as meson anti-meson mixing are briefly addressed. A detailed account of our conventions is deferred to appendix A.

* email: eherrmann@caltech.edu

¹ <http://europeanspallationsource.se/fundamental-and-particle-physics>

II. THE MODEL

We study one particular model with baryon-number violation but no proton decay, originally suggested in [12]. In a similar context, Babu et al. [13] discussed the role of color sextet scalars for non-supersymmetric gauge-coupling unification in a complete $SO(10)$ -theory, $n\bar{n}$ -oscillations and baryogenesis. Extending the analysis in [12, 13], we sharpen the link between $n\bar{n}$ -oscillations and baryogenesis. For our purposes, we focus on a simplified model with three additional scalars. The relevant degrees of freedom and their respective charges under $G_{SM} = SU(3)_c \times SU(2)_L \times U(1)_Y$ summarized in table I. The part of the color sextet Lagrangian relevant for

Field	$SU(3)_c$	$SU(2)_L$	$U(1)_Y$
X_1	$\bar{6}$	1	-1/3
X_2	$\bar{6}$	1	2/3
\tilde{X}_2	$\bar{6}$	1	2/3
Q_L	3	2	1/6
u_R	3	1	2/3
d_R	3	1	-1/3

TABLE I. Field content and respective representation under the Standard Model gauge group. Q_L represents a left-handed quark doublet and u_R , d_R are the right handed up- and down-type quarks.

baryogenesis and $n\bar{n}$ -oscillations takes the form²:

$$\begin{aligned} \mathcal{L}_{\text{sextet}} \supset & -g_1^{ab} X_1^{\alpha\beta} (Q_{L\alpha}^a \epsilon Q_{L\beta}^b) - g_2^{ab} X_2^{\alpha\beta} (d_{R\alpha}^a d_{R\beta}^b) \\ & - g_1^{ab} X_1^{\alpha\beta} (u_{R\alpha}^a d_{R\beta}^b) + \lambda X_1^{\alpha\alpha'} X_1^{\beta\beta'} X_2^{\gamma\gamma'} \epsilon_{\alpha\beta\gamma} \epsilon_{\alpha'\beta'\gamma'} \end{aligned} \quad (1)$$

In eq.(1), letters a, b , etc. denote the flavor structure, whereas greek letters α, β, \dots represent $SU(3)$ -color indices. Note that integrating out X_2 , which we assume to be heavy, would generate a quartic coupling for X_1 . This leads us to expect that the dimensionful coupling λ is of order M_2 , the mass of X_2 . Scalar sextets are represented as symmetric 3×3 -matrices in color space,

$$(X^{\alpha\beta}) = \frac{1}{\sqrt{2}} \begin{pmatrix} \sqrt{2}\tilde{X}^{11} & \tilde{X}^{12} & \tilde{X}^{13} \\ \tilde{X}^{12} & \sqrt{2}\tilde{X}^{22} & \tilde{X}^{23} \\ \tilde{X}^{13} & \tilde{X}^{23} & \sqrt{2}\tilde{X}^{33} \end{pmatrix}. \quad (2)$$

Group theoretic details and color-flow Feynman rules for color sextets are given in the appendices of Refs. [16, 17].

As written above, our model contains a vast number of free parameters. In the following, we restrict our discussion to the case, where the color sextet scalars only couple to the first generation of quarks. This reduces the number of Yukawa-couplings considerably. In order to generate a baryon

asymmetry via X_2 -decays (c.f. Feynman diagrams in fig.1), we have to introduce a second heavy sextet, \tilde{X}_2 with a Lagrangian analogous to eq.1 and couplings denoted by tildes. In Ref. [12] it was shown that even when X_2 and \tilde{X}_2 couple to one generation of quarks only, it is impossible to remove all CP -violating phases of the model by field redefinitions. The presence of CP -violation allows us to satisfy one of Sakharov's criteria so that X_2 -decays prefer matter over anti-matter. We will comment on the exact form and the relevant size of the CP -violating parameter later.

For the color sextets, we neglect all interactions in the scalar potential besides the cubic $\lambda, \tilde{\lambda}$ -terms. We choose $\lambda, \tilde{\lambda}$ to be real and move the phases to the Yukawa-couplings g_2 and \tilde{g}_2 . In the discussion on $n\bar{n}$ -oscillations, we also neglect g_1 , the coupling of X_1 to the left-handed quarks, so that we are left with the following set of parameters $\{M_1, M_2, \tilde{M}_2, g_2, \tilde{g}_2, \lambda, \tilde{\lambda}, g_1'\}$.

III. BARYOGENESIS

As discussed in the introduction, Sakharov [6] formulated three conditions for successful baryogenesis which we will discuss in the context of our model.

The standard assumption [18] of a baryon-symmetric big bang and the observational fact that there is more matter than anti-matter in the present Universe requires that baryon number has to be violated [6]. This is Sakharov's second condition. Nonperturbatively, the Standard Model has a source of baryon number violation in the form of instanton interactions [19, 20], which play a role in several baryogenesis scenarios, c.f. e.g. [1, 5]. However, we focus on a model that explicitly breaks B (and thereby also $(B-L)$) at tree level.

From the Lagrangian (1), it is easy to understand how this breaking takes place in our model. We envision a situation where one of the color sextets, X_1 , is much lighter³ than the other two, X_2 and \tilde{X}_2 . For the purpose of baryogenesis, we will treat X_1 as a stable particle ($g_1, g_1' \ll 1$). Its interactions with quarks dictate that X_1 has baryon number $-2/3$ and eventually decays hadronically. Looking at the $g_2 X_2 d_R d_R$ -term in eq.(1), we would also assign baryon number $-2/3$ to X_2 , which makes it impossible to consistently assign baryon number in the $\lambda X_1 X_1 X_2$ -term so that B is violated by X_2 -interactions.

We use a standard out of equilibrium decay of the heavy X_2 -scalars to satisfy Sakharov's last condition. In an expanding Universe, processes go out of equilibrium (freeze out), when their rate is small compared to the expansion rate dictated by the Hubble parameter H . High scale baryogenesis scenarios became somewhat unfashionable when people realized the tension between high reheating temperatures required for these models and predictions within simple inflationary

² We do not display the complete scalar potential nor parts of the Lagrangian involving the \tilde{X}_2 field, required to generate CP -violation. In terms of an $SO(10)$ -symmetric GUT-model there can be relations between different Yukawa couplings [13].

³ An additional light fundamental scalar aggravates the fine-tuning problem of the Standard Model which we do not address here. In the GUT-framework suggested in Ref.[13] it is preferred to have a light sextet to help with gauge coupling unification.

frameworks [5]. However, if one takes into account a mechanism termed *preheating* [21], GUT-scale reheating temperatures can be achieved.

A. Boltzmann equations

Boltzmann equations are a standard tool to accurately study the evolution of distribution functions and number densities in the early Universe. This is particularly important in parameter regions where simplified assumptions of a free evolution fail. In our model, the fields involved in the generation of the baryon asymmetry have a large color charge under the strong interaction which can lead to sizable reaction rates in comparison to the Hubble parameter. In order to explore the relation of successful baryogenesis and visible $n\bar{n}$ -oscillations reliably, we solve a coupled system of Boltzmann equations for the abundance of X_2 and the light species d , X_1 numerically.

In the following we list the relevant rate equations for our color sextet model. Notational details and definitions are deferred to appendix A. Our discussion of Boltzmann equations follows closely the expositions in Refs.[4, 22–24] including subtleties involving the real intermediate state (RIS) subtraction to avoid an overcounting of $2 \rightarrow 2$ -scattering contributions. In our calculation we work to lowest order and do not take finite temperature effects for propagators and coupling constants into account. For a discussion on finite temperature effects in the context of thermal leptogenesis, see [22].

For simplicity, we assume $\lambda/M_2, \tilde{\lambda}/M_2 \ll g_2, \tilde{g}_2$ so that the dominant contributions to baryon number violating X_2 -decays are given in the top line of figure 1. The relevant decay rates

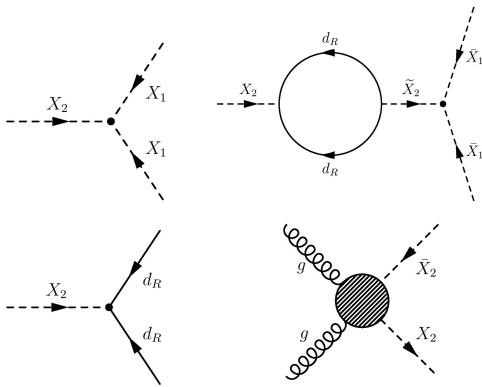


FIG. 1. Top: Baryon number violating $\Delta B = 2$ decays of X_2 at tree and one-loop level.

Bottom: We neglect a diagram with X_1 running in the loop, which is suppressed for $\lambda/M_2, \tilde{\lambda}/M_2 \ll g_2, \tilde{g}_2$. Tree level $2 \rightarrow 2$ -scattering processes between gluons and X_2 s which could contribute to washout effects, by keeping X_2 in equilibrium, are taken into account.

and scattering cross sections are given by⁴:

$$\Gamma(X_2 \rightarrow dd) = \frac{M_2 |g_2|^2}{16\pi}, \quad (3)$$

$$\Gamma(X_2 \rightarrow \bar{X}_1 \bar{X}_1) = \frac{3\lambda}{8\pi M_2} \left[\lambda - \tilde{\lambda} \frac{M_2^2 \Im[g_2^\dagger \tilde{g}_2]}{4\pi(M_2^2 - \tilde{M}_2^2)} \right], \quad (4)$$

$$\Gamma(\bar{X}_2 \rightarrow X_1 X_1) = \frac{3\lambda}{8\pi M_2} \left[\lambda + \tilde{\lambda} \frac{M_2^2 \Im[g_2^\dagger \tilde{g}_2]}{4\pi(M_2^2 - \tilde{M}_2^2)} \right], \quad (5)$$

$$\begin{aligned} \sigma(gg \rightarrow X_2 \bar{X}_2) = & \frac{\pi \alpha_s^2}{s^2} \frac{2C(2)_6 d_6}{d_8^2} \times \\ & \left[\frac{1}{6} \beta [6C(2)_6(4M_2^2 + s) + C(2)_8(10M_2^2 - s)] \right. \\ & \left. - \frac{4M_2^2}{s} [C(2)_8 M_2^2 + C(2)_6(s - 2M_2^2)] \ln \frac{1+\beta}{1-\beta} \right], \end{aligned}$$

where $\beta = \sqrt{1 - \frac{4M_2^2}{s}}$. The group theory constants are given in tab. II.

$R \triangleq d_R$	3	6	8
C_R	1/2	5/2	3
$C(2)_R$	4/3	10/3	3

TABLE II. Group theory constants for $SU(3)$ -multiplets. d_R is the dimension of the representation R . C_R denotes the Dynkin index $\text{Tr}[T_R^a T_R^b] = C_R \delta^{ab}$, whereas $C(2)_R$ represents the quadratic Casimir $\sum_a T_R^a T_R^a = C(2)_R \mathbb{1}_R$.

Following our notation of appendix A, we write the Boltzmann equation for X_2 ⁵:

$$\begin{aligned} sH(z)z \frac{dY_{X_2}(z)}{dz} = & -[X_2 \leftrightarrow \bar{X}_1 \bar{X}_1] - [X_2 \leftrightarrow d\bar{d}] + [gg \leftrightarrow X_2 \bar{X}_2] \\ = & \left[-\frac{Y_{X_2}}{Y_{X_2}^{eq}} + 1 \right] \gamma_D^{eq} + \left[-\frac{Y_{X_2} Y_{\bar{X}_2}}{Y_{X_2}^{eq} Y_{\bar{X}_2}^{eq}} + 1 \right] \gamma^{eq}(gg \rightarrow X_2 \bar{X}_2) \\ & - \frac{\bar{Y}_{X_1}}{Y_{X_1}^{eq}} Br \gamma_D^{eq} - \frac{\bar{Y}_d}{Y_d^{eq}} (1 - Br) \gamma_D^{eq}, \end{aligned} \quad (6)$$

and for \bar{X}_2 :

$$sH(z)z \frac{dY_{\bar{X}_2}(z)}{dz} = -[\bar{X}_2 \leftrightarrow X_1 X_1] - [\bar{X}_2 \leftrightarrow dd] + [gg \leftrightarrow X_2 \bar{X}_2]$$

⁴ Here we give the results in terms of rates where we **averaged** over spins and colors in the initial state and **summed** over final state quantum numbers. However, we express the Boltzmann equations in terms of initial **and** final state summed rates [22]. The results for the sextet-gluon scattering rate can also be found in [25, 26].

⁵ We neglected all terms of order $O(\epsilon^2)$ and measure temperatures with respect to M_2 by introducing the dimensionless parameter $z = M_2/T$. We write all rates as thermally averaged quantities γ_i^{eq} , c.f. App.A.

$$\begin{aligned}
&= \left[-\frac{Y_{\bar{X}_2}}{Y_{X_2}^{eq}} + 1 \right] \gamma_D^{eq} + \left[-\frac{Y_{X_2} Y_{\bar{X}_2}}{Y_{X_2}^{eq} Y_{X_2}^{eq}} + 1 \right] \gamma^q(gg \rightarrow X_2 \bar{X}_2) \\
&+ \frac{\bar{Y}_{X_1}}{Y_{X_1}^{eq}} Br \gamma_D^{eq} + \frac{\bar{Y}_d}{Y_d^{eq}} (1 - Br) \gamma_D^{eq}.
\end{aligned} \quad (7)$$

In eq.(6) we have defined the following quantities:

$$\bar{Y}_{X_1} \equiv Y_{X_1} - Y_{\bar{X}_1}, \quad (8)$$

$$\bar{Y}_d \equiv Y_d - Y_{\bar{d}}, \quad (9)$$

$$\epsilon \equiv \frac{\gamma^{eq}(X_2 \rightarrow \bar{X}_1 \bar{X}_1) - \gamma^{eq}(\bar{X}_2 \rightarrow X_1 X_1)}{\gamma^{eq}(X_2 \rightarrow \bar{X}_1 \bar{X}_1) + \gamma^{eq}(\bar{X}_2 \rightarrow X_1 X_1)}, \quad (10)$$

$$Br \equiv \frac{\gamma^{eq}(X_2 \rightarrow \bar{X}_1 \bar{X}_1)}{\gamma^{eq}(X_2 \rightarrow \bar{X}_1 \bar{X}_1) + \gamma^{eq}(X_2 \rightarrow \bar{d} \bar{d})}, \quad (11)$$

$$\gamma_D^{eq} \equiv \gamma^{eq}(X_2 \rightarrow \bar{X}_1 \bar{X}_1) + \gamma^{eq}(X_2 \rightarrow \bar{d} \bar{d}). \quad (12)$$

Note that \bar{Y}_{d,X_1} is zero in thermal equilibrium, so that all source terms in the Boltzmann equation vanish and the particle number for X_2 does not change in co-moving coordinates as expected. Throughout this work, we measure temperatures with respect to M_2 and define the dimensionless variable $z = M_2/T$. Assuming that X_2 decays only into X_1 and d , we have additional relations between the decay rates:

$$\frac{\gamma^{eq}(X_2 \rightarrow \bar{d} \bar{d})}{\gamma_D^{eq}} = 1 - Br, \quad (13)$$

$$\frac{\gamma^{eq}(\bar{X}_2 \rightarrow X_1 X_1)}{\gamma_D^{eq}} = \frac{1 - \epsilon}{1 + \epsilon} Br, \quad (14)$$

$$\frac{\gamma^{eq}(\bar{X}_2 \rightarrow dd)}{\gamma_D^{eq}} = 1 - \frac{1 - \epsilon}{1 + \epsilon} Br. \quad (15)$$

In order not to overestimate washout effects, we need to take into account real intermediate state subtraction (RIS) for the light species [22–24]. The Boltzmann equations for the asymmetry of the light particles $\bar{Y}_{X_1} = Y_{X_1} - Y_{\bar{X}_1}$ and $\bar{Y}_d = Y_d - Y_{\bar{d}}$ are expressed in terms of unsubtracted quantities only.

$$\begin{aligned}
z H s \frac{d\bar{Y}_{X_1}}{dz} &= -2 \left[\frac{Y_{X_2} - Y_{\bar{X}_2}}{Y_{X_2}^{eq}} Br \gamma_D^{eq} + \left(\frac{Y_{\bar{X}_2}}{Y_{X_2}^{eq}} - 1 \right) \epsilon Br \gamma_D^{eq} \right] \\
&+ 4 \left[\left(1 + \frac{\bar{Y}_d}{Y_d^{eq}} \right) \gamma^{eq}(dd \rightarrow X_1 X_1) - \left(1 + \frac{\bar{Y}_{X_1}}{Y_{X_1}^{eq}} \right) \gamma^{eq}(X_1 X_1 \rightarrow dd) \right. \\
&\left. - \frac{\bar{Y}_{X_1}}{Y_{X_1}^{eq}} Br^2 \gamma_D^{eq} - \frac{\bar{Y}_d}{Y_d^{eq}} (1 - Br) Br \gamma_D^{eq} \right]
\end{aligned} \quad (16)$$

$$\begin{aligned}
z H s \frac{d\bar{Y}_d}{dz} &= -2 \left[\frac{Y_{X_2} - Y_{\bar{X}_2}}{Y_{X_2}^{eq}} (1 - Br) \gamma_D^{eq} - \left(\frac{Y_{\bar{X}_2}}{Y_{X_2}^{eq}} - 1 \right) \epsilon Br \gamma_D^{eq} \right] \\
&- 4 \left[\left(1 + \frac{\bar{Y}_d}{Y_d^{eq}} \right) \gamma^{eq}(dd \rightarrow X_1 X_1) - \left(1 + \frac{\bar{Y}_{X_1}}{Y_{X_1}^{eq}} \right) \gamma^{eq}(X_1 X_1 \rightarrow dd) \right. \\
&\left. + \frac{\bar{Y}_{X_1}}{Y_{X_1}^{eq}} (1 - Br) Br \gamma_D^{eq} + \frac{\bar{Y}_d}{Y_d^{eq}} (1 - Br)^2 \gamma_D^{eq} \right]
\end{aligned} \quad (17)$$

To obtain the total baryon yield we have to combine the contributions from X_1 and d ,

$$Y_B = \frac{1}{3} \bar{Y}_d - \frac{2}{3} \bar{Y}_{X_1}. \quad (18)$$

Before embarking on a numerical study of the Boltzmann evolution equations for the baryon asymmetry we wish to give a qualitative picture of our model by investigating various limits of the parameter space. An example of the relevant reaction rates that enter the Boltzmann equations is shown in fig. 2.

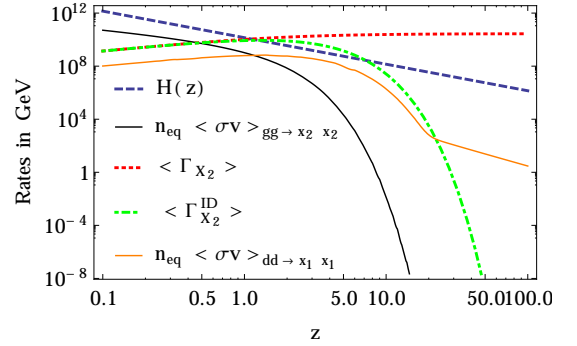


FIG. 2. For one representative parameter point, we show the relevant decay (Γ_{X_2}), inverse decay ($\Gamma_{X_2}^{ID}$) and scattering rates that enter into the Boltzmann equations. We chose $M_2 = 10^{14}$ GeV, $\lambda = 3.5 \times 10^{-2} M_2$ and $|g_2|^2 = 8.4 \times 10^{-2}$. Gluon scattering is not important and the dominant washout contribution comes from inverse decays that are active up to $z=5-10$. Varying these parameters can shift the relevant rates with respect to the Hubble parameter $H(z)$.

The quantitative behavior of these rates is well understood and can be found in standard textbooks on cosmology (c.f. e.g. [18]). For the sake of brevity, we will not repeat the discussion here with two exceptions. First, due to the large color charge of X_2 , one could think that its strong interactions with gluons keeps X_2 in equilibrium so that no baryon asymmetry can be generated. We demonstrate that this is generically not the case. And second, we discuss the decay rates of X_2 as they play a role in our discussions on $n\bar{n}$ -oscillations later.

- (a) Gluon interactions: $\Gamma_{gg \rightarrow X_2 \bar{X}_2} = n_g^{eq} \langle v \sigma(gg \rightarrow X_2 \bar{X}_2) \rangle$; We evaluate the thermal average, eq.(A7), numerically and compare it to the Hubble rate, eq.(A4). This constraint only depends on the strong coupling constant α_s and M_2 , the mass of X_2 . The numerical results are summarized in fig.3. Analytically, we can estimate the mass M_2^* for which the two rates are equal at the characteristic temperature $T = M_2 \Leftrightarrow z = 1$ and find $M_2^* \sim \frac{\alpha_s^2 M_{pl}}{\pi^2 g_{sS}^{1/2}}$. Using the RGE-evolved strong coupling constant α_s at the high scale, we find $M_2^* \sim 10^{13-14}$ GeV. Comparing $\Gamma_{gg \rightarrow X_2 \bar{X}_2}$ and H only at $z = 1$, one would conclude that gluon scattering keeps X_2 in thermal equilibrium for masses $M_2 < M_2^*$ because $n_g^{eq} \langle \sigma v \rangle|_{z=1} \sim M_2$ and the Hubble rate falls as $H \sim M_2^2$ at $z = 1$. However, this does not take into account the exponential Boltzmann

suppression once the temperature falls below the M_2 -threshold. In that case only gluons in the high energy tail of the distribution have sufficient energy to pair produce the X_2 . In the reverse process, the rate is proportional to the number density of X_2 which also follows a Boltzmann distribution for $T < M_2$. An example of this behavior can be seen in fig. 2. Only for low masses M_2 is it possible that the gluon interactions keep X_2 in equilibrium in a reasonable temperature range ($1 \lesssim z \lesssim 10$) so that the generation of baryon asymmetry is inhibited, c.f. fig.3.

- (b) Decays: $\langle \Gamma(X_2 \rightarrow \bar{X}_1 \bar{X}_1; \bar{d} \bar{d}) \rangle$; For this discussion it is useful to combine the two tree level decay channels of X_2 , eq.(3) and eq.(4) into the total decay rate. As discussed before, λ is dimensionful and should be of order $\lambda \sim M_2$ which is why we introduce the dimensionless coupling $\tilde{\lambda} = \lambda/M_2$. Parameterizing the total decay rate in terms of an effective interaction strength $\Gamma_{X_2} = \frac{1}{4} M_2 \alpha_{\text{eff}}$, where

$$\alpha_{\text{eff}} = \frac{|g_2|^2 + 6\tilde{\lambda}^2}{4\pi}, \quad (19)$$

we obtain the out of equilibrium relation

$$\alpha_{\text{eff}} < 1.66 \times g_{*S}^{1/2} M_2 / M_{pl}. \quad (20)$$

The requirement for the decay rates to satisfy the out of equilibrium conditions are not entirely sharp. In Ref.[18] an approximate analytic analysis of washout effects due to inverse decay processes and $2 \rightarrow 2$ -scattering processes can be found. If we introduce the ratio $K = \langle \Gamma_{X_2} \rangle|_{z=1} / 2H(1)$ by which the out of equilibrium conditions are violated, one has to include a damping factor for the free out of equilibrium result $Y_B^{\text{free}} = 2\epsilon Br / g_{*S}$, so that [18]

$$Y_B^{\text{imp}} \approx Y_B^{\text{free}} \times \frac{0.3}{K(\ln K)^{0.6}}, \text{ if } K > 1. \quad (21)$$

For very large K , when baryon number violating $2 \rightarrow 2$ -scatterings are important, the washout factor decreases the final baryon asymmetry exponentially[18]. We visualize the interesting parameter region for baryogenesis by comparing the Hubble rate $H(z=1)$ with the relevant annihilation cross section $n_{X_2}^{eq} \langle \sigma(gg \rightarrow X_2 \bar{X}_2) \rangle$ as well as thermally averaged decay rate⁶ $\langle \Gamma_{X_2} \rangle = \frac{K_1(z)}{K_2(z)} \Gamma_{X_2}$ in the M_2 - α_{eff} -plane in fig. 3. The main focus in the following paragraphs lies in a numerical treatment of the Boltzmann equations to correctly take washout effects into account beyond the analytical approximations. This also highlights the fact that not all parameters that give a correct baryon yield in the free out of equilibrium approximation, $Y_B = 2\frac{\epsilon Br}{g_{*S}}$, are viable. In our treatment, we improve previous discussions of high scale baryogenesis within the color sextet model found in Refs. [12, 13].

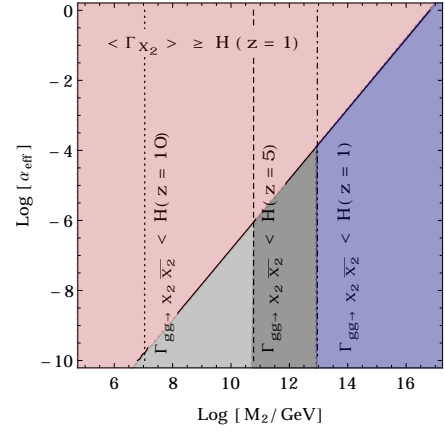


FIG. 3. Estimate of allowed mass range and coupling strength for X_2 from baryogenesis considerations.

Contours indicate $\langle \Gamma_{X_2} \rangle|_{z=1} = H(z=1)$ and $\Gamma_{gg \rightarrow X_2 \bar{X}_2} \equiv n_g^{eq} \langle \sigma(gg \rightarrow X_2 \bar{X}_2) \rangle|_{z=z^*} = H(z^* = 1, 5, 10)$, where the thermally averaged reaction rates equal the Hubble rate. The red region represents parameter points where the X_2 -decay rate is dominant. The effective decay strength α_{eff} is related to our model parameters via eq. 19.

B. Reducing number of model parameters

Our model in its general form has a large number of free parameters. In addition to the coupling constants, we have the masses of the $(\sim) X_2$ -fields, $(\sim) M_2$ (treating the quarks and X_1 massless for the purpose of baryogenesis).

Exploring the full parameter range of the model including all phases is a formidable task which is beyond the scope of this work. In the one-family limit described in Sec. II, our model does not contribute new sources to meson- anti-meson mixing. Even if we relaxed this assumption, the large X_2 -mass helps to satisfy the limits from $K^0 \bar{K}^{(0)}$ -mixing for example.

The relevant parameters for baryogenesis are the CP -violating parameter ϵ , eq.(10), and the branching fraction Br , eq.(11) which reduce to ⁷:

$$\epsilon = \frac{\tilde{\lambda}}{\lambda} \frac{1}{4\pi} \frac{M_2^2 \Im[g_2^\dagger \tilde{g}_2]}{\tilde{M}_2^2 - M_2^2}, \quad (22)$$

$$Br = \frac{3\tilde{\lambda}^2}{\frac{1}{2}|g_2|^2 + 3\tilde{\lambda}^2}. \quad (23)$$

We combine the phase $\Im[g_2^\dagger \tilde{g}_2]$, the mass ratio of the heavy sextets and the ratio of the trilinear couplings into a single effective CP -violating parameter ϵ . Within this simplified framework, we ask which model parameters give a baryon

⁶ $K_i(z)$ denote the modified Bessel functions.

⁷ Instead of the phase $\Im[g_2^\dagger \tilde{g}_2]$ and the mass ratio \tilde{M}_2^2/M_2^2 , we mostly work with the effective parameter ϵ that characterizes CP -violation.

yield Y_B ⁸ consistent with experiment [28] $Y_B = \frac{n_B - n_{\bar{B}}}{s} = (8.75 \pm 0.23) \times 10^{-11}$. To estimate the range of viable model parameters, we insert eq.(22) and eq.(23) into the free out of equilibrium decay result which relates the baryon yield Y_B to ϵ and Br ,

$$Y_B^{\text{free}} = 2 \frac{\epsilon Br}{g_{*S}} = \frac{2}{g_{*S}} \epsilon \times \frac{3\bar{\lambda}^2}{\frac{1}{2}|g_2|^2 + 3\bar{\lambda}^2}, \quad (24)$$

which is essentially independent of M_2 ⁹. This approximation is valid in parameter regions where all annihilation and decay rates of the baryon number violating X_2 are comparably smaller than Hubble $H(z=1)$.

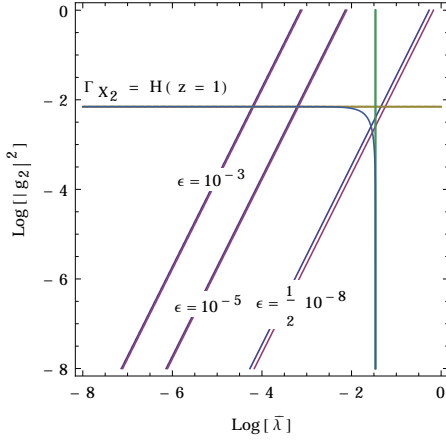


FIG. 4. Parameter region consistent with the experimental value $Y_B = (8.75 \pm 0.23) \times 10^{-11}$ using the free out of equilibrium decay estimate. CP -violation is characterized by a single parameter, ϵ . The additional contours indicate where the Hubble rate at $z=1$ equals the decay rates $\Gamma_{X_2 \rightarrow d\bar{d}}$ (horizontal lines) and $\Gamma_{X_2 \rightarrow \tilde{X}_1 \tilde{X}_1}$ (vertical lines) for $M_2 = 10^{14}$ GeV.

C. Numerical Results for Baryon Asymmetry

Following the general considerations and the analytical estimates of parameter regions, where baryogenesis is feasible, we show numerical results for the coupled system of Boltzmann equations where a free decay scenario is not applicable. We verified that our numerical results agree with analytic estimates in the free out of equilibrium decay regime of the model (large M_2 , small α_{eff}).

In order to investigate the influence of the decay rate of X_2 relative to the Hubble rate, we increase the cubic scalar coupling λ together with g_2 gradually so that the free out of equilibrium conditions are not satisfied any more. To make the results

comparable, we keep ϵ and Br constant. Doing so, the free out of equilibrium calculation tells us that the baryon yield $Y_B = 2\epsilon Br/g_{*S}$ remains constant as well. We also compare our numerical results to the improved analytical solution given in eq.(21) if applicable. Starting with a parameter point, where the coupling constants are chosen so that the decay rates are equal to the Hubble rate,

$$M_2 = 10^{14} \text{ GeV}, \quad \tilde{M}_2 = 2 M_2,$$

$$\bar{\lambda}^2 = \frac{8\pi}{3} 1.66 g_*^{1/2} \frac{M_2}{M_{pl}} = (0.034)^2, \quad \tilde{\lambda} = \lambda,$$

$$|g_2|^2 = 16\pi 1.66 g_*^{1/2} \frac{M_2}{M_{pl}} = 0.007, \quad \Im[g_2^\dagger \tilde{g}_2] = 0.1 |g_2|^2,$$

$$\epsilon = 1.8 \times 10^{-5},$$

$$Br = 0.5,$$

and increasing α_{eff} , eq.(19), by factors of 10 corresponds to a violation of one of Sakharov's conditions [6]. As expected, for large $K = \langle \Gamma_{X_2} \rangle / 2H(1)$, the net baryon asymmetry decreases considerably. For fig.5, we keep ϵ , Br and M_2 fixed, so that $Y_B^{\text{free}} = \frac{2\epsilon Br}{g_{*S}} \approx 1.8 \times 10^{-7}$ is constant.

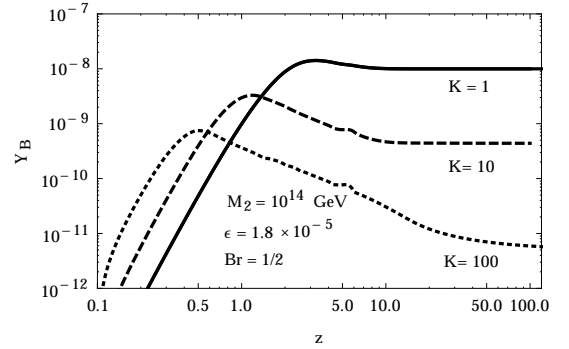


FIG. 5. Numerical result of baryon asymmetry Y_B for different X_2 -decay rates. We adjusted the parameters such that ϵ and Br remain constant. Large values of $K = \Gamma_{X_2}/2H(z=1)$ keep X_2 in equilibrium longer which leads to washout effects at large z .

K	Y_B^{free}	Y_B^{imp}	Y_B^{num}
1	1.8×10^{-7}	—	9.9×10^{-9}
10	1.8×10^{-7}	3.2×10^{-9}	4.3×10^{-10}
100	1.8×10^{-7}	9.7×10^{-11}	5.9×10^{-12}

TABLE III. Comparison between free out of equilibrium (Y_B^{free}), washout improved analytical (Y_B^{imp} , eq.(21)) and numerical (Y_B^{num}) results for the baryon asymmetry.

Note that the results in tab.III show that our numerical results can vary up to a factor of ten from the washout corrected analytic results Y_B^{imp} , eq.(21). We also increased the CP -violating parameter ϵ and found roughly linear dependence. The same is true when the branching fraction Br is varied. In fact, our model reproduces all aspects of the high scale toy model for baryogenesis discussed in Ref. [4].

⁸ The yield Y_B is related to the commonly quoted baryon to photon ration [27] $\eta = \frac{n_B - n_{\bar{B}}}{n_\gamma} = (6.19 \pm 0.14) \times 10^{-10}$.

⁹ M_2 and \tilde{M}_2 are expected to be of the same size, so that we can parameterize $R = \tilde{M}_2/M_2$ and the overall scale drops out in ϵ

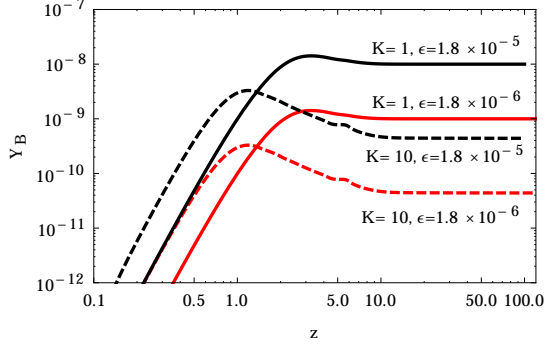


FIG. 6. Comparing numerical results for the baryon asymmetry for different K and ϵ , keeping $M_2 = 10^{14}$ GeV fixed. We find excellent agreement with the expectations of Ref. [4].

IV. $n\bar{n}$ -OSCILLATIONS

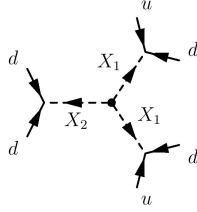


FIG. 7. Contribution to $n\bar{n}$ -oscillations via $\Delta B = 2$ process involving the scalar sextet fields.

Neutron anti-neutron oscillation experiments can directly probe the structure of baryon number violation [29, 30]. In comparison to proton decay experiments which probe $\Delta B = 1, \Delta L$ odd-modes (e.g. $p \rightarrow e^+ \pi^0$), $n\bar{n}$ -oscillations are intimately related to $\Delta B = 2$ processes. Future experiments such as the European Spallation Source (ESS) could push the bounds on this mode of matter instability to $\tau \approx 10^{36}$ years¹⁰ exceeding current limits on the proton lifetime $\tau_p > 8.2 \times 10^{33}$ years [11]. A number of models that predict $n\bar{n}$ -oscillations have been considered in the past, c.f. e.g. [12, 13, 31–33]. The fact that $n\bar{n}$ -oscillations require baryon number violation suggests that the underlying dynamics of these low energy processes can be linked to baryogenesis as pointed out by Kuzmin [31] and others. In the presence of a TeV-scale colored scalar, $n\bar{n}$ -oscillation experiments can probe energy scales up to 10^{15-16} GeV [12], which we take to be the scale of baryon number violating interactions via X_2 -decays. Light color sextet scalars, such as X_1 ($M_1 \sim \text{few TeV}$), can be present in non-supersymmetric $SO(10)$ -models that lead to gauge coupling unification as described in detail in [13]. In the previous section we focused on a careful treatment of baryogenesis by solving Boltzmann equations numerically.

Here we are going to relate these results to the discovery potential of $n\bar{n}$ -oscillations in present and future experiments.

Neutron-anti-neutron oscillation experiments are sensitive to the transition matrix element $\Delta m = \langle \bar{n} | \mathcal{H}_{\text{eff}} | n \rangle$. The effective low energy Hamiltonian \mathcal{H}_{eff} for $n\bar{n}$ -transitions in our model is given in Ref. [12]¹¹. Neglecting the Yukawa-coupling to left-handed quarks, g_1 , Δm is characterized by [12]

$$\Delta m = 2\lambda\beta^2 \frac{|(g'_1)^2 g_2|}{3M_1^4 M_2^2}, \quad (25)$$

where $\beta = 0.01 \text{ GeV}^3$ has been determined in lattice gauge theory [34]. The current limit on $n\bar{n}$ -oscillations is given by [35] $\Delta m < 2 \times 10^{-33}$ GeV and could be improved by a few orders of magnitude in suggested future experiments¹².

If we restrict ourselves to the one-family scenario, we can express Δm in terms of the decay rates by substituting λ and g_2 .

$$\Delta m = 2\beta^2 \sqrt{\frac{128\pi^2}{3}} \sqrt{Br(1-Br)} \frac{|g'_1|^2}{3M_2^2 M_1^4} \Gamma_{X_2}. \quad (26)$$

For successful baryogenesis, the X_2 s have to decay out of equilibrium. This is only possible if the $K = \Gamma_{X_2}/2H(z=1)$ -factor as defined in the previous section is not larger than $O(100)$ for a CP -violating parameter $\epsilon \approx 10^{-5}$. Taking this into account, we can relate successful baryogenesis to $n\bar{n}$ -oscillations by setting $\Gamma_{X_2} < K \times H(1) = K \times 1.66 g_{*S}^{1/2} M_2^2/M_{pl}$. With this substitution M_2 drops out of Δm , and we get an upper bound on the transition rate:

$$\Delta m < \frac{2\beta^2 \times 1.66 g_{*S}^{1/2}}{3M_{pl}} \sqrt{\frac{128\pi^2}{3}} \sqrt{Br(1-Br)} \frac{|g'_1|^2}{M_1^4} K. \quad (27)$$

Written in this form, Δm is tied to Br and K which directly enter our baryogenesis analysis described above. One is left with parameters that concern the light sextet X_1 . This allows us to consistently combine $n\bar{n}$ -oscillations, baryogenesis and LHC-phenomenology for our color sextet model. For M_1 around the TeV-scale one can search for signals of this particle at the LHC. In principle, we might be able to measure its coupling g'_1 to u_R, d_R -quarks picking out one particular point in fig.8. We comment on possible collider signals in the next section. Note that there is some tension between demanding visible $n\bar{n}$ -oscillations in the future, successful baryogenesis and collider constraints. Even for $Br = 1/2$, where $\sqrt{Br(1-Br)}$ is maximized, a K -factor of 1 is almost completely excluded. Increasing K to larger values, it becomes important to take

¹¹ A similar result was obtained in [13]

¹² In [36], four orders of magnitude improvements on the free oscillation probability (corresponds to two orders of magnitude in Δm) are estimated for a 1MW spallation target at Project X. The limits for ESS should be at least comparable.

¹⁰ <http://europeanspallationsource.se/fundamental-and-particle-physics>

washout effects of the baryon asymmetry into account and one is forced to go beyond the free out of equilibrium decay scenario used in [12].

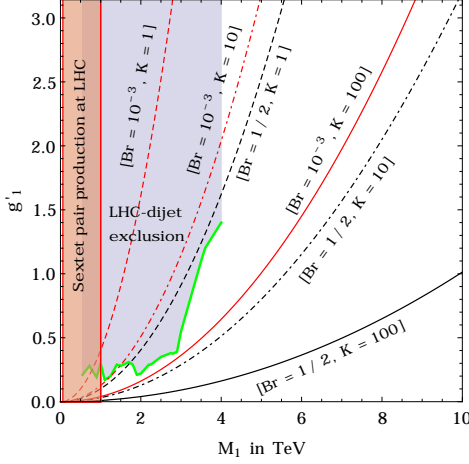


FIG. 8. Contourplot of Δm in the $g'_1 - M_1$ -plane for different values of $K = \Gamma_{X_2}/2H(1)$ and branching fraction Br of X_2 . Different contours represent values where Δm as written in eq.(27) is equal to the expected sensitivity of future $n\bar{n}$ -oscillation experiments, $\Delta m^{\text{fut}} = 10^{-35}$ GeV. Note that current limits on $n\bar{n}$ -oscillations can easily be avoided if the decay rate Γ_{X_2} is small, there is no obstruction from baryogenesis. If we see $n\bar{n}$ -oscillations in near future experiments, the allowed parameter region is to the upper left of the contours. We also include collider limits on color sextets from LHC-dijet searches that have been analyzed in Ref. [15]. The orange contour represents the simulated limits for color sextet pair production at the 14 TeV LHC with $\mathcal{L} = 100 \text{ fb}^{-1}$ integrated luminosity.

V. CONSTRAINTS FROM NEUTRON ELECTRIC DIPOLE MOMENTS AND COLLIDERS

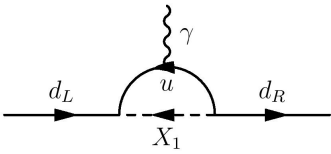


FIG. 9. Down-quark contribution to the electric dipole moment of the neutron.

Since our model includes additional sources of CP -violation, in principle we have to worry about contributions to quark electric dipole moments (EDMs) coming from diagrams such as fig. 9. Using $SU(6)$ -wavefunctions, the quark EDMs are related to the dipole moment of the neutron d_N by, $d_N = \frac{4}{3}d_d - \frac{1}{3}d_u \simeq \frac{4}{3}d_d$ [37]. In the Standard Model, quark EDMs are first generated at 3-loop [37] and are additionally suppressed by the GIM -mechanism leading to a prediction for

the neutron-EDM of¹³ $d_N = O(10^{-34})$ e cm. The current experimental bound is given in [39], $d_N^{\text{exp}} < 5.5 \times 10^{-26}$ e cm. The tiny Standard Model contributions allow us to estimate limits for our model parameters. Specifically, we obtain restrictions on g'_1 from X_1 contributions to the down-quark-EDM via the diagram shown in fig. 9. For a nonzero g_1 (so far we used $g_1 = 0$) in the one generation approximation, the leading contribution of X_1 to the electric dipole moment of the down-quark is given by[12]:

$$|d_d| \simeq \frac{m_u}{6\pi^2 M_1^2} \log\left(\frac{M_1^2}{m_u^2}\right) |\Im[g_1(g'_1)^*]| \text{ e cm.} \quad (28)$$

If we use the QCD scale $\Lambda_{\text{QCD}} \approx 1$ GeV instead of m_u we estimate,

$$|\Im[g_1(g'_1)^*]| \lesssim 8 \times 10^{-3}, \quad (29)$$

for $M_1 = 2$ TeV. Assuming that g_1 is comparable to g'_1 and there are no small phases in this sector, eq.(29) suggests, that $g'_1 = O(0.1)$. Comparing this to the parameter region preferred by baryogenesis and visible $n\bar{n}$ -oscillations points towards a light M_1 , c.f. fig. 8.

The production cross sections and decay rates of color sextet scalars have been studied intensively at tree and loop level, c.f. e.g.[16, 25, 40–42] and references therein. Depending on the range of couplings and mass of the sextet, either single- or pair-production can be dominant. Most of the work focuses on scalar sextets with Standard Model quantum numbers $\Phi \sim (6, 1, 4/3)$ which leads to same-sign top pair production via an s-channel exchange[40]. However, a majority of the results such as production cross sections or decay rates for these scalars can be extended to different quantum numbers [41]. We are interested in the LHC-phenomenology of $X_1 \sim (\bar{6}, 3, -1/3)$ which couples to $u_R d_R$ rather than $u_R u_R$. In terms of single scalar production, both cases should be comparable as the suppression of the down-quark parton distribution function is compensated by the combinatorics of the u, d initial state[16]. In our model with X_1 in the $(\bar{6}, 1, -1/3)$ -representation, the expected signals entail a resonance in the invariant dijet mass distribution (single production) or two equal mass dijets (pair production)[15]. Note that the authors of Ref. [15] obtained limits on the diquark mass of 1 TeV by simulating $\mathcal{L} = 100 \text{ fb}^{-1}$ integrated luminosity for the 14 TeV LHC by considering the pair production channel from gluons. This analysis is independent of the unknown sextet Yukawa-couplings and gives the pair production limit in fig.8.

More interesting for us at this point is the pure dijet analysis (single production) for a sextet in the $(6, 1, 4/3)_{\text{SM}}$ -representation in the same article¹⁴. As a final result they

¹³ Taking long distance effects of a six quark operator into account, Ref.[38] finds $d_N = O(10^{-31})$ e cm.

¹⁴ [42] use higher statistics dijet data from ATLAS and CMS to set similar limits on what we call g_1 and g'_1 but only consider masses up to 2 TeV.

show exclusion plots for the coupling of the scalar sextet to right-handed quarks ($u_R u_R$) depending on the mass of the sextet. Since no special features of the $u_R u_R$ channel such as same sign tops were used in their analysis, we convert their limits to our g'_1 - M_1 -plane. In fig. 8 we compared the collider limits with the estimates of $n\bar{n}$ -oscillations. To reiterate our conclusion from before; In parameter regions that are not excluded by LHC-searches it is possible to achieve visible $n\bar{n}$ -oscillations and successful baryogenesis. However, washout effects are important and a simple out of equilibrium calculation for the baryon asymmetry is not applicable.

VI. CONCLUSION

We studied a minimal model that leads to baryon number violation at tree level but no proton decay. This theory has been suggested in [12] and a similar field content was studied in connection to non-supersymmetric gauge coupling unification in [13]. The model contains a novel color sextet scalar at the TeV-scale ($X_1 \sim (\bar{6}, 1, -1/3)$) as well as two additional scalar sextets at a scale of $O(10^{14-15})$ TeV ($X_2, \tilde{X}_2 \sim (\bar{6}, 1, 2/3)$). In this setup, oscillations between neutrons and anti-neutrons are one of the primary signals of baryon number violating physics. Since baryon number violation is also one of the key ingredients to explain baryogenesis, it is natural to investigate potential connections between these two phenomena. With this motivation and the fact that the sextet scalars have large color charges, we studied a system of coupled Boltzmann equations to accurately predict the evolution of the baryon asymmetry in the early Universe in regimes where simple analytic results are not available. We were able to relate $n\bar{n}$ -oscillations to baryogenesis in such a way that only two high scale parameters Br , the branching ratio of the decay $X_2 \rightarrow \bar{X}_1 \bar{X}_1$ and the out of equilibrium factor $K = \Gamma_{X_2}/2H(1)$ enter the analysis. Taking into account collider constraints on the light sextet X_1 we demonstrated that, if we see $n\bar{n}$ -oscillations at future experiments, such as the suggested European Spallation Source (ESS), washout effects for baryogenesis become important. This is summarized in fig.8.

VII. ACKNOWLEDGEMENT

We thank Mark Wise for detailed discussions throughout the project and careful reading of the manuscript. We also acknowledge useful comments by Pavel Fileviez Perez, David Sanford and Yue Zhang. This work is supported by the DOE Grant # DE-SC0011632.

Appendix A: Details of Boltzmann equations

In this appendix, we collect a number of well known formulas relevant for our Boltzmann equations (6, 7, 16, 17). Most of this material is a summary of Refs. [4, 22–24]. In the presence of fast elastic scattering events, the particle species are kept in *kinetic* equilibrium. In this regime, the

phase space distribution functions can be approximated by a Maxwell-Boltzmann distribution. Each particle species is then characterized by its chemical potential μ_i or by its total abundance n_i respectively. These quantities can only be altered by inelastic processes. If these occur fast enough, *chemical* equilibrium will be maintained and the number- and energy-densities follow their equilibrium values n_i^{eq} and ρ_i^{eq} respectively. The phase space integral can be evaluated exactly. For Maxwell-Boltzmann statistics, one finds [4]¹⁵:

$$\begin{aligned} n_{MB}^{eq} &= g_i \int \frac{d^3 p}{(2\pi)^3} f^{eq}(p) = \int \frac{d^3 p}{(2\pi)^3} e^{-(E_i - \mu_i)/T} \\ &= g_i \int \frac{d^3 p}{(2\pi)^3} \exp \left[-(\sqrt{\vec{p}^2 + m_i^2} - \mu_i)/T \right] \\ &= g_i \frac{T^3}{2\pi^2} e^{-\mu_i/T} z_i^2 K_2(z_i), \end{aligned}$$

where $z_i = m_i/T$. The high- and low-temperature expansion is:

$$n_{MB}^{eq} = \begin{cases} g_i \left(\frac{mT}{2\pi} \right)^{3/2} e^{-(m-\mu)/T} \left[1 + \frac{15}{8z} + \dots \right], & m \gg T \\ g_i \frac{T^3}{\pi^2} e^{\mu/T} \left[1 - \frac{1}{4} z^2 + \dots \right], & m \ll T \end{cases} \quad (A1)$$

g_i counts the number of internal degrees of freedom of a given species (e.g. $g_\gamma = 2$, $g_{\text{glue}} = 8 \times 2 = 16$, etc). In *kinetic* equilibrium the phase space density is conveniently parameterized as

$$f(p) = f^{eq}(p) \frac{n}{n^{eq}}. \quad (A2)$$

Following the notation of [22, 23], the Boltzmann equation describing the time evolution of abundance n_X of some species X is:

$$\dot{n}_X + 3Hn_X = - \sum_{a,i,j} \Delta_s [X \ a \cdots \leftrightarrow i \ j \cdots], \quad (A3)$$

where the Hubble rate written in terms of z :

$$H = \frac{\dot{a}}{a} = \sqrt{\frac{8\pi\rho}{3m_{pl}}} = 1.66 g_{*S}^{1/2} \frac{T^2}{m_{pl}} = 1.66 g_{*S}^{1/2} \frac{m_X^2}{m_{pl}} \frac{1}{z^2}. \quad (A4)$$

Δ_s denotes a symmetry factor which depends on the number of X particles that are created or destroyed in a particular reaction, e.g. $\Delta_s = 2$ for a reaction $XX \rightarrow ij$.

In the definition of the Hubble rate, we encounter the effective number of degrees of freedom g_{*S} that contribute to the energy density ρ of the Universe. Since the relevant epoch is radiation dominated, it counts the relativistic degrees of freedom at a given temperature [18]. The Standard Model field content

¹⁵ Results for Fermi-Dirac and Bose-Einstein statistics can be found in the appendix of [4].

leads to $g_{*S} = 106.75$ above the electroweak phase transition, but gets modified by new relativistic species that are in thermal equilibrium (in our case this would be the light X_1 -field for example).

In eq.(A3) we defined

$$[X a \cdots \leftrightarrow i j \cdots] \equiv \frac{n_X n_{a \cdots}}{n_X^{eq} n_{a \cdots}^{eq}} \gamma_{eq}(X a \cdots \rightarrow i j \cdots) - \frac{n_i n_{j \cdots}}{n_i^{eq} n_{j \cdots}^{eq}} \gamma_{eq}(i j \cdots \rightarrow X a \cdots). \quad (\text{A5})$$

The $\gamma_{eq}(ab \cdots \rightarrow cd \cdots)$ denote thermally averaged reaction rates for a given process ($ab \cdots \rightarrow cd \cdots$). In the context of Boltzmann equations for baryogenesis, one often encounters the special cases of particle decay and $2 \rightarrow 2$ -scattering. The results for these processes are given by [22–24]¹⁶:

$$\begin{aligned} \gamma_{eq}(X \rightarrow ij) &= \int \frac{d^3 p_X}{(2\pi)^3 2E_X} f_X^{eq}(p_X) \frac{d^3 p_i}{(2\pi)^3 2E_i} \frac{d^3 p_j}{(2\pi)^3 2E_j} \times \\ &\quad (2\pi)^4 \delta^{(4)}(p_X - p_i - p_j) |M(X \rightarrow ij)|^2 \\ &= n_X^{eq} \frac{K_1(z)}{K_2(z)} \Gamma_X, \end{aligned} \quad (\text{A6})$$

where Γ_X is the decay width in the rest system of the particle summed over all initial **and** final state spins and colors. $K_1(z)$ and $K_2(z)$ denote the Bessel K -functions. Introducing the Lorentz-invariant measure $\widetilde{d^3 p} \equiv \frac{d^3 p}{(2\pi)^3 2E_p}$, the thermally averaged 2-body scattering rate is given by¹⁷:

$$\begin{aligned} \gamma_{eq}(Xa \rightarrow ij) &= \int \widetilde{d^3 p_X} \int \widetilde{d^3 p_a} f_X^{eq}(p_X) f_a^{eq}(p_a) \int \widetilde{d^3 p_i} \int \widetilde{d^3 p_j} \times \\ &\quad (2\pi)^4 \delta^{(4)}(p_X + p_a - p_i - p_j) |M(Xa \rightarrow ij)|^2 \end{aligned}$$

$$= \frac{T}{32\pi^4} \int_{s_{min}}^{\infty} ds s^{3/2} \lambda(1, M_X^2/s, M_a^2/s) \sigma(s) K_1\left(\frac{\sqrt{s}}{T}\right). \quad (\text{A7})$$

$\sigma(s)$ is the total cross section summed over all initial **and** final state spins and colors. $\lambda(a, b, c) = (a - b - c)^2 - 4bc$ is the usual kinematic function. s denotes the Mandelstam variable and $s_{min} = \max[(m_X + m_a)^2, (m_i + m_j)^2]$ picks out the threshold energy for a given process.

In order to absorb the dilution of particle species due to the expansion of the Universe reflected in the Hubble term $3Hn_X$ (cf. eq.(A3)), it is convenient to introduce comoving coordinates, $Y_i = n_i/s$, where the entropy density of the Universe, s , can be expressed as:

$$s = \frac{2\pi^2}{45} g_{*S}(T) T^3 = \frac{2\pi^2}{45} g_{*S}(T) \frac{m_X^3}{z^3}, \quad (\text{A8})$$

with the *effective number of degrees of freedom in entropy*

$$g_{*S}(T) = \sum_{i=\text{bosons}} g_i \left(\frac{T_i}{T}\right)^3 + \frac{7}{8} \sum_{i=\text{fermions}} g_i \left(\frac{T_i}{T}\right)^3. \quad (\text{A9})$$

When **all** relativistic species are in equilibrium at the same temperature one obtains $g_{*S}(T) = g_*$. Furthermore, we prefer to write the Boltzmann equations in terms of z instead of time t . In these variables the Boltzmann equation (A3) becomes:

$$zH(z)s(z) \frac{dY_X}{dz} = - \sum_{a,i,j} \Delta_s [X a \cdots \leftrightarrow i j \cdots]. \quad (\text{A10})$$

-
- [1] A. G. Cohen, D. Kaplan, and A. Nelson, *Ann.Rev.Nucl.Part.Sci.* **43**, 27 (1993), arXiv:hep-ph/9302210 [hep-ph].
[2] M. Luty, *Phys.Rev.* **D45**, 455 (1992).
[3] I. Affleck and M. Dine, *Nucl.Phys.* **B249**, 361 (1985).
[4] E. W. Kolb and S. Wolfram, *Nucl.Phys.* **B172**, 224 (1980).
[5] A. Riotto, , 326 (1998), arXiv:hep-ph/9807454 [hep-ph].
[6] A. Sakharov, *Pisma Zh.Eksp.Teor.Fiz.* **5**, 32 (1967).
[7] P. Huet and E. Sather, *Phys.Rev.* **D51**, 379 (1995), arXiv:hep-ph/9404302 [hep-ph].
[8] H. Georgi and S. Glashow, *Phys.Rev.Lett.* **32**, 438 (1974).
[9] S. Dimopoulos and H. Georgi, *Nucl.Phys.* **B193**, 150 (1981).
[10] J. C. Pati and A. Salam, *Phys.Rev.* **D10**, 275 (1974).
[11] H. Nishino *et al.* (Super-Kamiokande Collaboration), *Phys.Rev.Lett.* **102**, 141801 (2009), arXiv:0903.0676 [hep-ex].

- [12] J. M. Arnold, B. Fornal, and M. B. Wise, *Phys.Rev.* **D87**, 075004 (2013), arXiv:1212.4556 [hep-ph].
[13] K. Babu and R. Mohapatra, *Phys.Lett.* **B715**, 328 (2012), arXiv:1206.5701 [hep-ph].
[14] S. Peggs, R. Calaga, R. Duperrier, J. Stovall, M. Eshraqi, *et al.*, (2009).
[15] P. Richardson and D. Winn, *Eur.Phys.J.* **C72**, 1862 (2012), arXiv:1108.6154 [hep-ph].
[16] T. Han, I. Lewis, and T. McElmurry, *JHEP* **1001**, 123 (2010), arXiv:0909.2666 [hep-ph].
[17] W. Kilian, T. Ohl, J. Reuter, and C. Speckner, *JHEP* **1210**, 022 (2012), arXiv:1206.3700 [hep-ph].
[18] E. W. Kolb and M. S. Turner, *Front.Phys.* **69**, 1 (1990).
[19] G. 't Hooft, *Phys.Rev.* **D14**, 3432 (1976).
[20] P. B. Arnold and L. D. McLerran, *Phys.Rev.* **D36**, 581 (1987).
[21] P. B. Greene, L. Kofman, A. D. Linde, and A. A. Starobinsky, *Phys.Rev.* **D56**, 6175 (1997), arXiv:hep-ph/9705347 [hep-ph].
[22] G. Giudice, A. Notari, M. Raidal, A. Riotto, and A. Strumia, *Nucl.Phys.* **B685**, 89 (2004), arXiv:hep-ph/0310123 [hep-ph].
[23] A. Strumia, , 655 (2006), arXiv:hep-ph/0608347 [hep-ph].
[24] W. Buchmuller, P. Di Bari, and M. Plumacher, *Annals Phys.* **315**, 305 (2005), arXiv:hep-ph/0401240 [hep-ph].

¹⁶ $\gamma_{eq}(X \rightarrow ij)$ is related to the thermally averaged decay rate $\langle \Gamma(X \rightarrow ij) \rangle$ via $\gamma_{eq}(X \rightarrow ij) = n_X^{eq} \langle \Gamma(X \rightarrow ij) \rangle$.

¹⁷ The second step is valid if the cross section only depends on s and not on the thermal motion relative to the background plasma [22]. γ^{eq} is related to the thermally averaged cross section via $\langle v\sigma(ab \rightarrow X) \rangle = n_a^{eq} n_b^{eq} \gamma^{eq}(ab \rightarrow X)$.

- [25] C.-R. Chen, W. Klemm, V. Rentschler, and K. Wang, *Phys.Rev.* **D79**, 054002 (2009), arXiv:0811.2105 [hep-ph].
- [26] A. V. Manohar and M. B. Wise, *Phys.Rev.* **D74**, 035009 (2006), arXiv:hep-ph/0606172 [hep-ph].
- [27] C. Bennett *et al.* (WMAP), *Astrophys.J.Suppl.* **208**, 20 (2013), arXiv:1212.5225 [astro-ph.CO].
- [28] K. Babu and R. Mohapatra, *Phys.Rev.Lett.* **109**, 091803 (2012), arXiv:1207.5771 [hep-ph].
- [29] Y. A. Kamyshkov, (2002), arXiv:hep-ex/0211006 [hep-ex].
- [30] R. Mohapatra, *J.Phys.* **G36**, 104006 (2009), arXiv:0902.0834 [hep-ph].
- [31] V. Kuzmin, *Pisma Zh.Eksp.Teor.Fiz.* **12**, 335 (1970).
- [32] Z. Chacko and R. Mohapatra, *Phys.Rev.* **D59**, 055004 (1999), arXiv:hep-ph/9802388 [hep-ph].
- [33] B. Dutta, Y. Mimura, and R. Mohapatra, *Phys.Rev.Lett.* **96**, 061801 (2006), arXiv:hep-ph/0510291 [hep-ph].
- [34] N. Tsutsui *et al.* (CP-PACS Collaboration, JLQCD Collaborations), *Phys.Rev.* **D70**, 111501 (2004), arXiv:hep-lat/0402026 [hep-lat].
- [35] K. Abe *et al.* (Super-Kamiokande Collaboration), (2011), arXiv:1109.4227 [hep-ex].
- [36] K. Babu, S. Banerjee, D. Baxter, Z. Berezhiani, M. Bergevin, *et al.*, (2013), arXiv:1310.8593 [hep-ex].
- [37] A. Czarnecki and B. Krause, *Phys.Rev.Lett.* **78**, 4339 (1997), arXiv:hep-ph/9704355 [hep-ph].
- [38] T. Mannel and N. Uraltsev, *Phys.Rev.* **D85**, 096002 (2012), arXiv:1202.6270 [hep-ph].
- [39] A. Serebrov, E. Kolomenskiy, A. Pirozhkov, I. Krasnosheikova, A. Vasiliev, *et al.*, (2013), arXiv:1310.5588 [nucl-ex].
- [40] R. Mohapatra, N. Okada, and H.-B. Yu, *Phys.Rev.* **D77**, 011701 (2008), arXiv:0709.1486 [hep-ph].
- [41] E. L. Berger, Q.-H. Cao, C.-R. Chen, G. Shaughnessy, and H. Zhang, *Phys.Rev.Lett.* **105**, 181802 (2010), arXiv:1005.2622 [hep-ph].
- [42] Y. C. Zhan, Z. L. Liu, S. A. Li, C. S. Li, and H. T. Li, *Eur.Phys.J.* **C74**, 2716 (2014), arXiv:1305.5152 [hep-ph].